

S1

Supporting Information for

Smartly designed photoreactive silica nanoparticles and their reactivity.

by

Anna Peled, Maria Naddaka and Jean-Paul Lellouche

S2

Supporting information

Table of Contents

List of abbreviations	S3
Literature compounds	S4
Experimental Procedures and characterization data	S5-S7
^1H - and ^{13}C - NMR Spectra	S7-S10
TGA	S10
Solid state ^{13}C and ^{29}Si CP-MAS NMR spectra	S11
UV absorbance spectra	S12-S13
FT-IR spectra	S13
Size distribution graphs	S14-S15
SEM tilt images	S16-S17
AFM images	S18
AFM NP manipulation images	S19-S21
SEM and AFM images of neat PC film	S22
XPS	S23-S25
Fluorescence images	S26
Literature	S27

S3

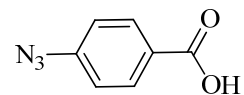
List of abbreviations:

AFM	atomic force microscopy
APTES	(3-aminopropyl)triethoxysilane
CDI	1,1'-carbonyldiimidazole
CP-MAS	cross polarization-magic angle spinning
DLS	dynamic light scattering
DMAP	para-dimethylaminopyridine
DMSO	dimethylsulfoxide
DSS	4,4-dimethyl-4-silapentane-1-sulfonic acid
EtOH	ethanol
FE	field emission
FIB	focused ion beam
FTIR	fourier transform infrared spectroscopy
HRMS	high resolution mass spectra
NMR	nuclear magnetic resonance
RT	room temperature
SEM	scanning electron microscope
ssNMR	solid state nuclear magnetic resonance
TEOS	tetraethyl orthosilicate
THF	tetrahydrofurane
TMS	tetramethylsilane
TEM	transmission electron spectroscopy
UV	ultra violet
XPS	X-ray photoelectron spectroscopy

S4

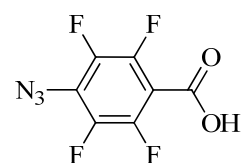
Literature compounds:

4-azidobenzoic acid



The 4-azidobenzoic acid was prepared according to a literature procedure.^[1]

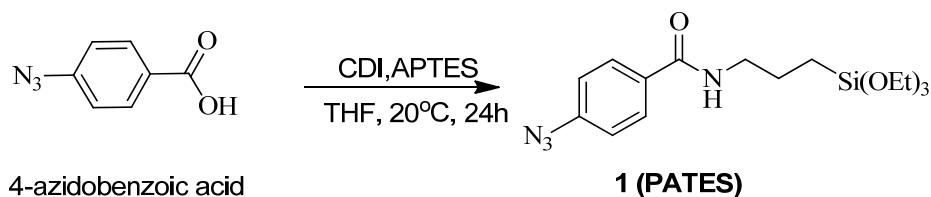
4-azido-2,3,5,6-tetrafluorobenzoic acid



The 4-azido-2,3,5,6-tetrafluorobenzoic acid was prepared according to a literature procedure.^[2]

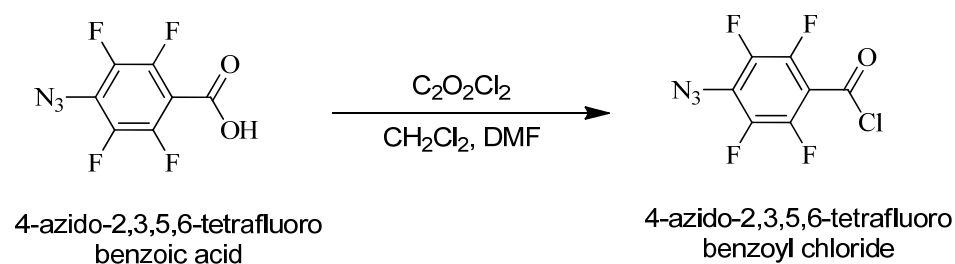
Experimental Procedures:

Synthesis of 4-azido-N-(3-(triethoxysilyl)propyl)benzamide **1** (PATES)



Yellow oil; TLC, $R_f = 0.24$ (eluent: acetone /*n*-hexane: 85/15); ν_{\max} (KBr easy diff)/ cm^{-1} 3322 (NH), 2973 and 2885 (CH stretching), 2927 (CH_2 stretching), 2124 (azide), 1639 (C=O amide), 1549 and 1287 (C=C), 1287 (C-O), 1445 and 765 (CH_2 bending), 1390 (Si-O CH_2CH_3), 1100 (Si-O), 956 (C-O); δ_{H} ^1H NMR (300 MHz; DMSO- d_6) 8.48 (1H, br t, NH), 7.91 (2H, d, $J = 8.7$ Hz, Ar-H), 7.17 (2H, d, $J = 8.7$ Hz, Ar-H), 3.74 (6H, q, $J = 6.9$ Hz, O- CH_2 -CH $_3$), 3.27-3.21 (2H, m, NH- CH_2 -CH $_2$), 1.64-1.54 (2H, m, CH $_2$ -CH $_2$ -CH $_2$), 1.13 (9H, t, $J = 6.9$ Hz, O-CH $_2$ -CH $_3$), 0.61-0.56 (2H, m, CH $_2$ -Si); δ_{C} ^{13}C NMR (75 MHz, [D $_6$] DMSO, TMS) 165.1 (C), 142.0 (C), 131.3 (C), 129.0 (CH), 118.7 (CH), 57.7 (CH $_2$), 42.0 (CH $_2$), 22.7 (CH $_2$), 18.1 (CH $_3$), 7.4 (CH $_2$); UV/Vis λ_{\max} (EtOH)/nm (270); HRMS (DCI+ CH $_4$) m/z calcd for $\text{C}_{16}\text{H}_{26}\text{N}_4\text{O}_4\text{Si}$ (MH) $^+$ 366.4875 found 366.1723.

Synthesis of 4-azido-2,3,5,6-tetrafluorobenzoyl chloride

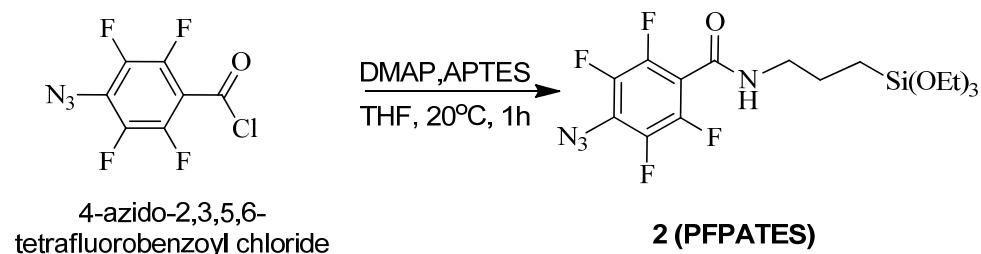


The 4-azido-2,3,5,6-tetrafluorobenzoic acid (2.20 g, 9.36 mmol) was dissolved in dry CH_2Cl_2 (10 mL). In order to dissolve 4-azido-2,3,5,6-tetrafluorobenzoic acid completely dry DMF (0.3 mL) was added to a reaction mixture. Thus oxalyl chloride (3.6 mL, 42.12 mmol) was added and reaction was stirred at RT for 2h during which time gas evolution was observed. After reaction completion the solvents were evaporated to give 4-azido-2,3,5,6-tetrafluorobenzoyl chloride as yellow oil which was directly used in the next step without further purification.

S6

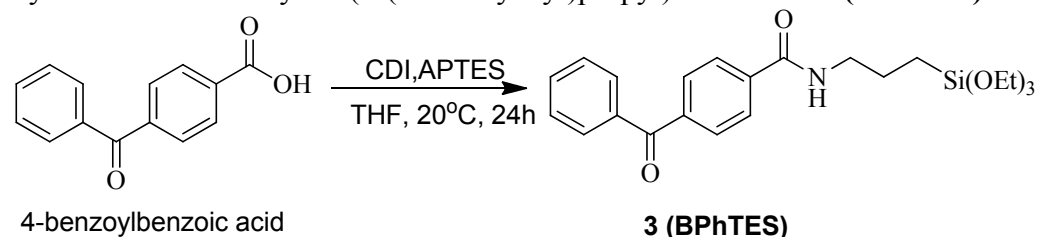
Synthesis of 4-azido-2,3,5,6-tetrafluoro-N-(3-(triethoxysilyl)propyl)benzamide

2 (PFPATES)



Yellow oil; TLC, $R_f = 0.37$ (eluent: ether/n-hexane: 60/40); ν_{\max} (KBr easy diff)/ cm^{-1} 3280 (NH), 3080 and 2884 (CH stretching), 2930 (CH_2 stretching), 2133 (azide), 1650 (C=O amide), 1392 (Si-OCH₂CH₃), 1100 (Si-O), 958 (C-O), 777 (CH_2 bending); δ_{H} ¹H NMR (300 MHz, CDCl₃) 6.42 (1H, br t, NH), 3.81 (6H, q, $J = 6.9$ Hz, O-CH₂-CH₂), 3.51-3.44 (2H, m, NH-CH₂-CH₂), 1.81-1.71 (2H, m, CH₂-CH₂-CH₂), 1.21 (9H, t, $J = 6.9$ Hz, O-CH₂-CH₃), 0.73-0.66 (2H, m, CH₂-Si); δ_{C} ¹³C NMR (75 MHz; CDCl₃) 157.4 (C), 145.7 (C), 142.1 (C), 138.7 (C), 112.1 (C), 58.5 (CH₂), 42.4 (CH₂), 22.5 (CH₂), 18.2 (CH₃), 7.6 (CH₂); δ_{F} ¹⁹F NMR (188 MHz; CDCl₃) 141.3-141.5 (m, 2F), 150.9-151.1 (m, 2F); UV/Vis λ_{\max} (EtOH)/nm (260); HRMS (DCI+ CH₄) m/z calcd for C₁₆H₂₂F₄N₄O₄Si (MH-EtOH)⁺ 393.3810 found 393.1006.

Synthesis of 4-benzoyl-N-(3-(triethoxysilyl)propyl)benzamide **3 (BPhTES)**



¹HNMR was identical to previously reported. [3]

White solid; TLC, $R_f = 0.68$ (eluent: acetone /n-hexane: 85/15); m.p. 90-91°C; ν_{\max} (KBr easy diff)/ cm^{-1} 3326 (NH), 2975 and 2885 (CH stretching), 2928 (CH_2 stretching), 1663 (C=O ketone), 1631 (C=O amide), 1553 (C=C), 1445 and 790 (CH_2 bending), 1390 (Si-OCH₂CH₃), 1300 (C-H bending), 1278 and 1108 (C-O), 1167 (C-N), 1080 (Si-O) cm^{-1} ; δ_{H} ¹H NMR (300 MHz, [D₆] DMSO, TMS) 8.68 (1H, br t, NH), 8.02-7.98 (2H, m, Ar-H), 7.78-7.68 (5H, m, Ar-H),

S7

7.61-7.56 (2H, m, Ar-H), 3.77 (6H, q, $J = 9.6$ Hz, O-CH₂-CH₃), 3.35-3.25 (2H, m, NH-CH₂-CH₂), 1.67-1.57 (2H, m, CH₂-CH₂-CH₂), 1.15 (9H, t, $J = 9.6$ Hz, O-CH₂-CH₃), 0.65-0.59 (2H, m, CH₂-Si); δ_c ¹³C NMR (75 MHz, [D₆] DMSO, TMS) 195.4 (C), 165.3 (C), 139.0 (C), 138.0 (C), 136.7 (C), 133.0 (CH), 129.7 (CH), 129.5 (CH), 128.7 (CH), 127.3 (CH), 57.7 (CH₂), 42.1 (CH₂), 22.7 (CH₂), 18.2 (CH₃), 7.5 (CH₂); UV/Vis λ_{\max} (EtOH)/nm (260); HRMS (DCI+ CH₄) m/z calcd for C₂₃H₃₁NO₅Si (MH)⁺ 429.5814 found 430.248.

¹H- and ¹³C- NMR Spectra:

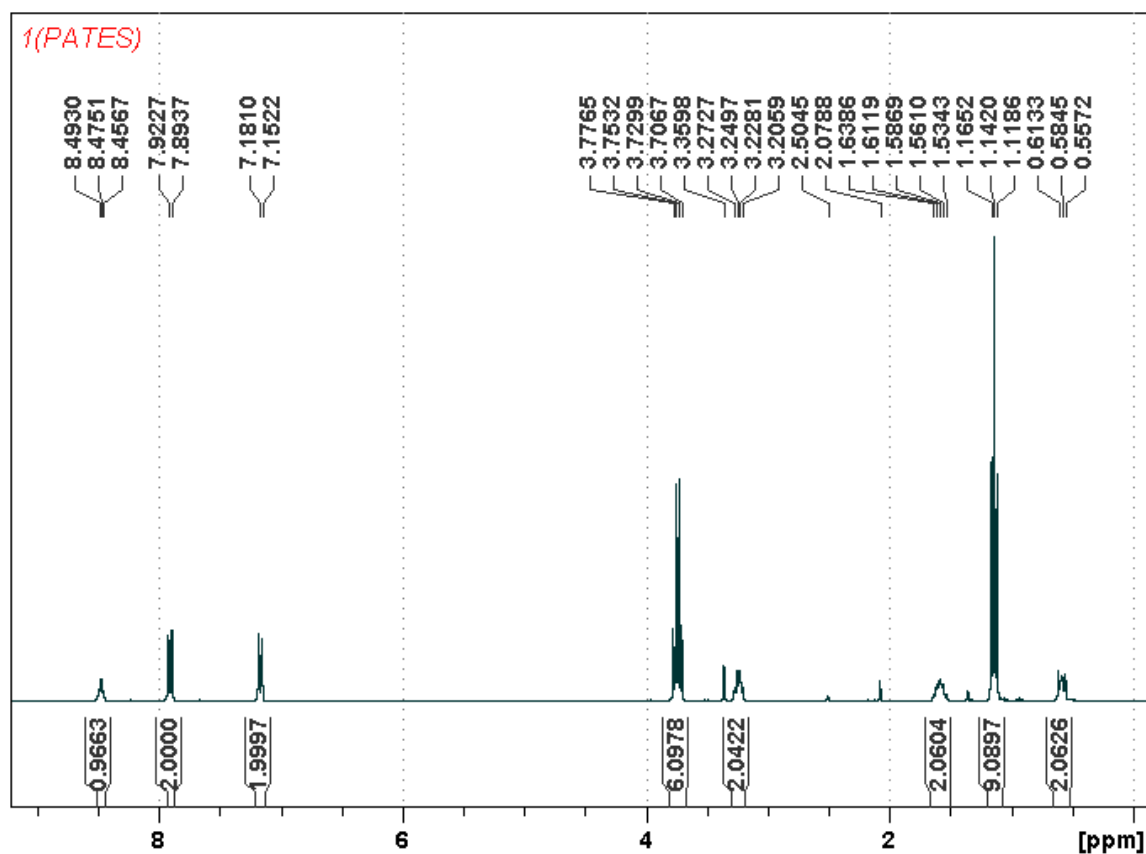


Figure 1. ¹H NMR spectrum of 1 (PATES)

S8

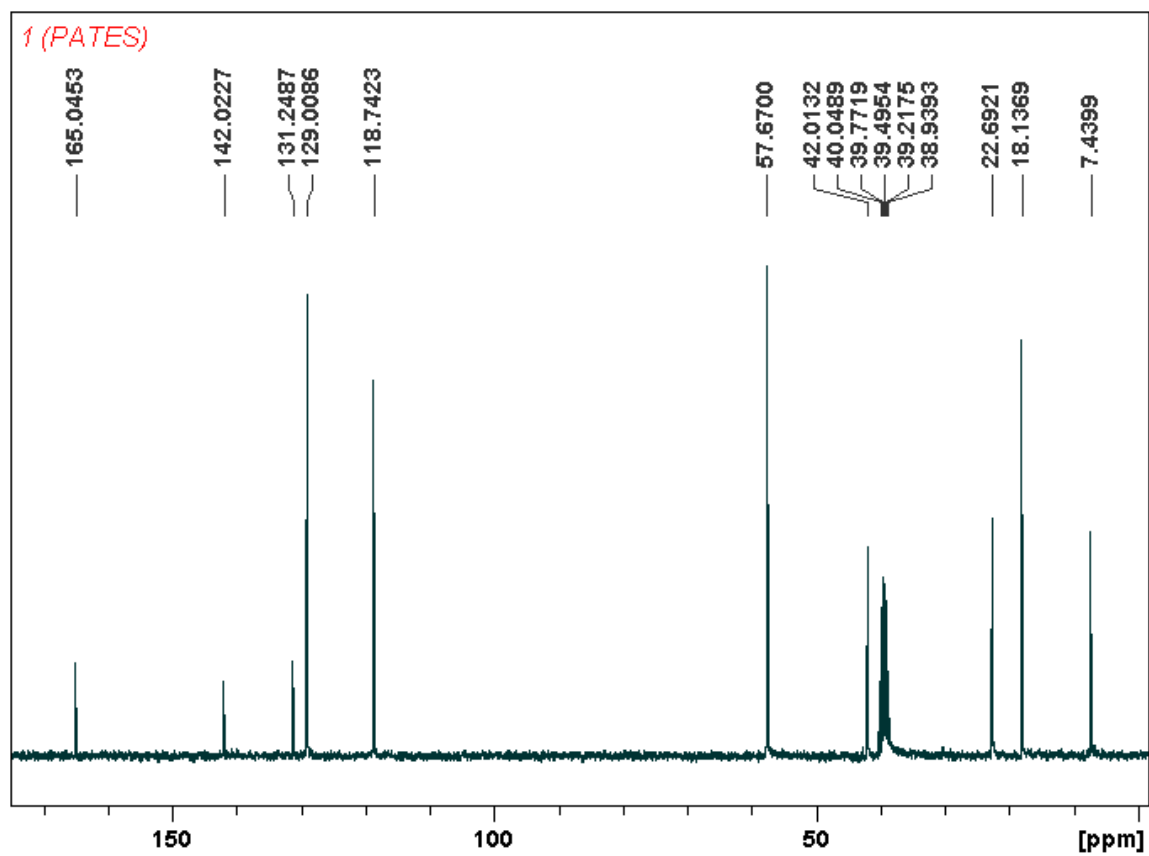


Figure 2. ^{13}C NMR spectrum of 1 (PATES)

S9

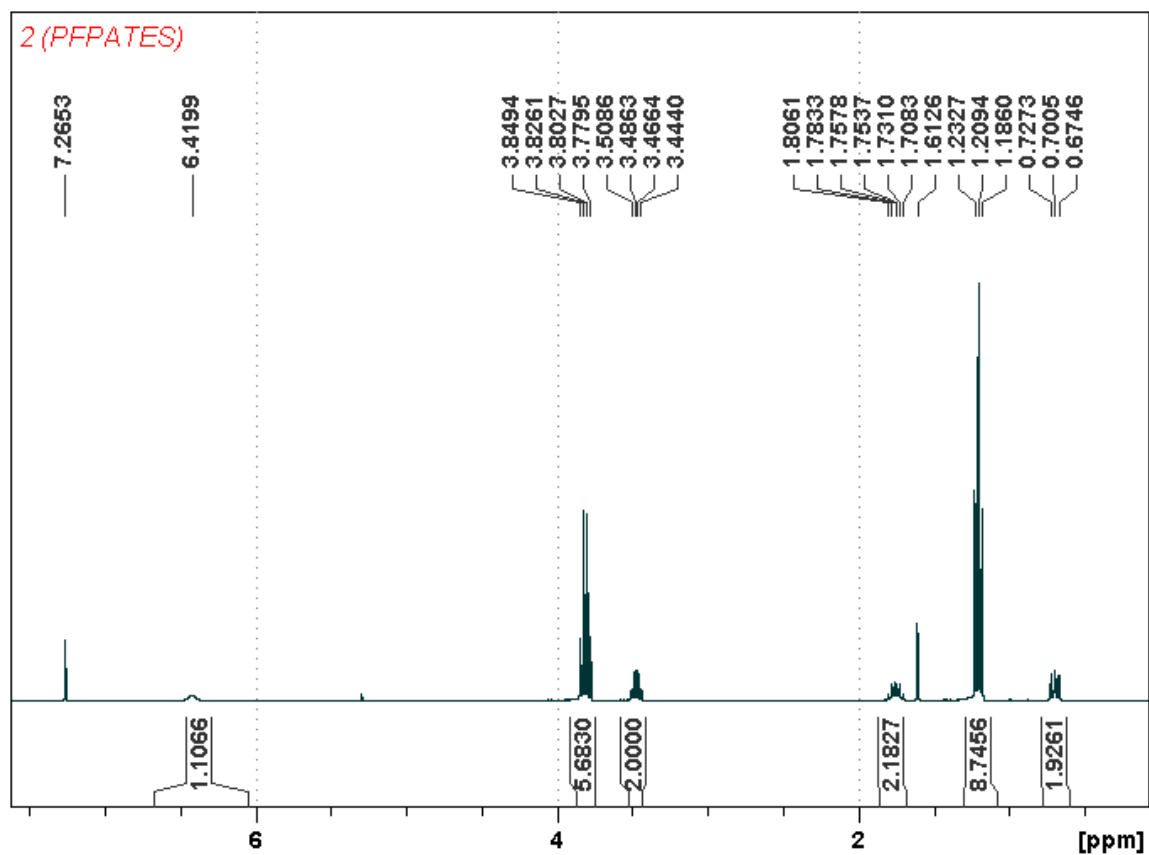


Figure 3. ^1H NMR spectrum of **2** (PFPATES)

S10

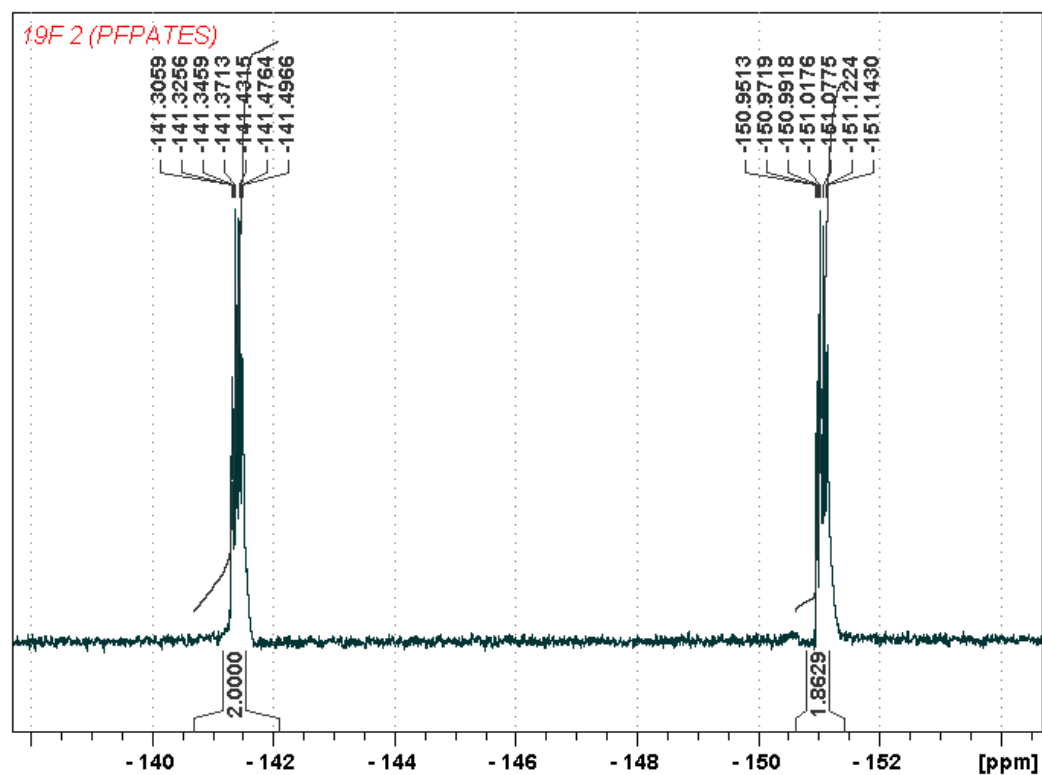


Figure 4. ¹⁹F NMR spectrum of 2 (PFPATES)

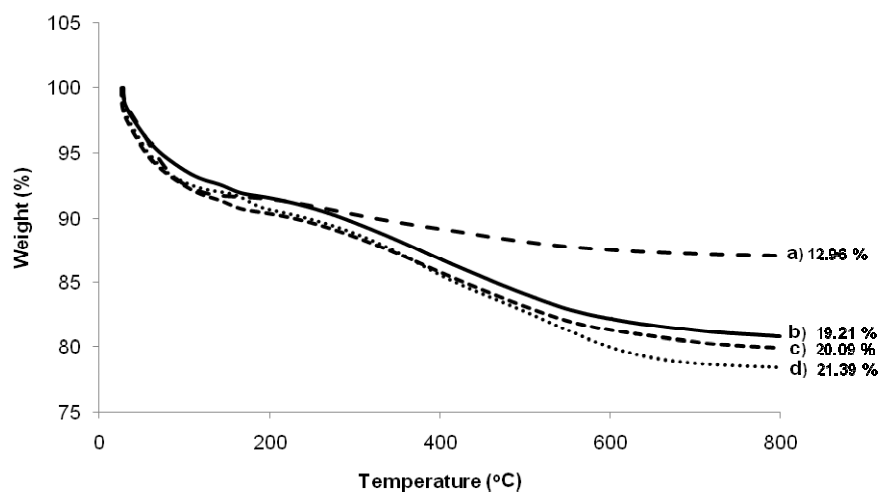


Figure 5. TGA of a) SiO₂, b) SiO₂@BPh, c) SiO₂@PFPA, d) SiO₂@PA NPs. TGA was performed in air at a heating rate of 10 °C/min

S11

Solid state ^{13}C and ^{29}Si CP-MAS NMR spectra:

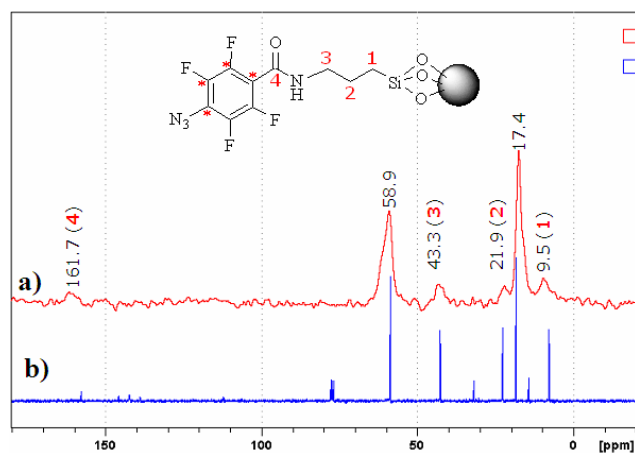


Figure 6. a) ^{13}C CP/MAS NMR spectrum of the SiO_2 @PFPA NPs; b) ^{13}C NMR (75 MHz; CDCl_3) spectrum of **2** (PFPA-TES)

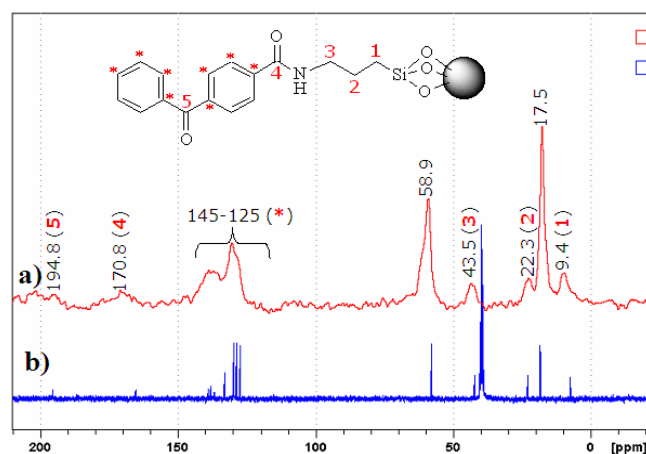


Figure 7. a) ^{13}C CP/MAS NMR spectrum of the SiO_2 @BPh NPs; b) ^{13}C NMR (75 MHz; $[\text{D}_6]$ DMSO) spectrum of **3** (BPh-TES)

S12

UV absorbance spectra:

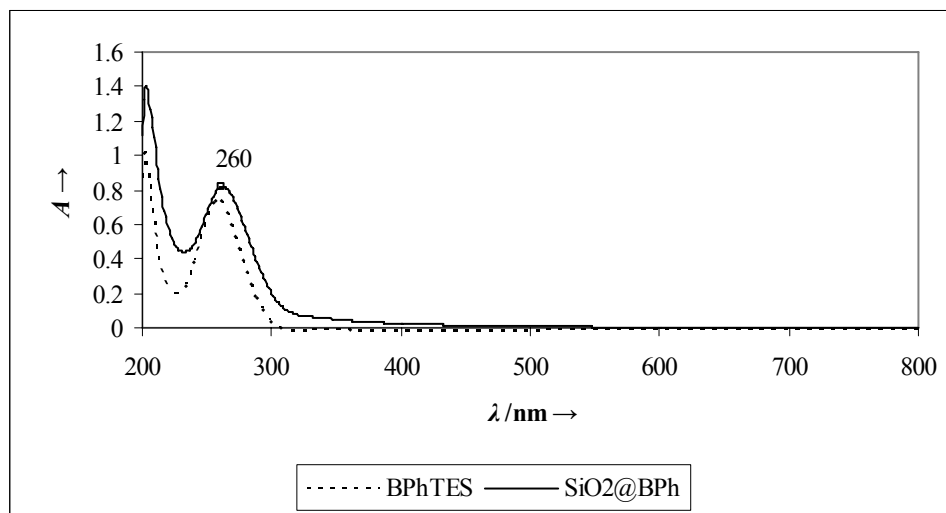


Figure 8. UV/Vis spectra of the **3** (BPhTES) and SiO₂@BPh NPs

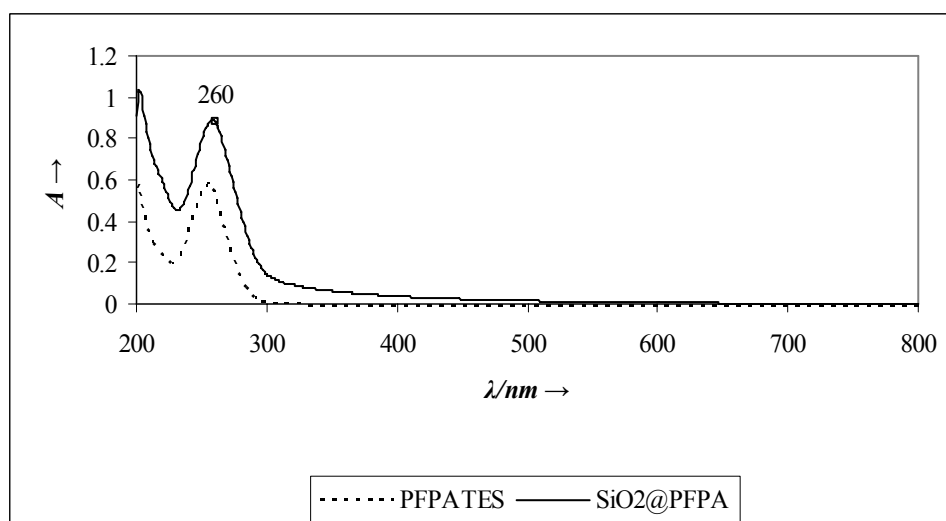


Figure 9. UV/Vis spectra of the **2** (PFPATES) and SiO₂@PFPA NPs

S13

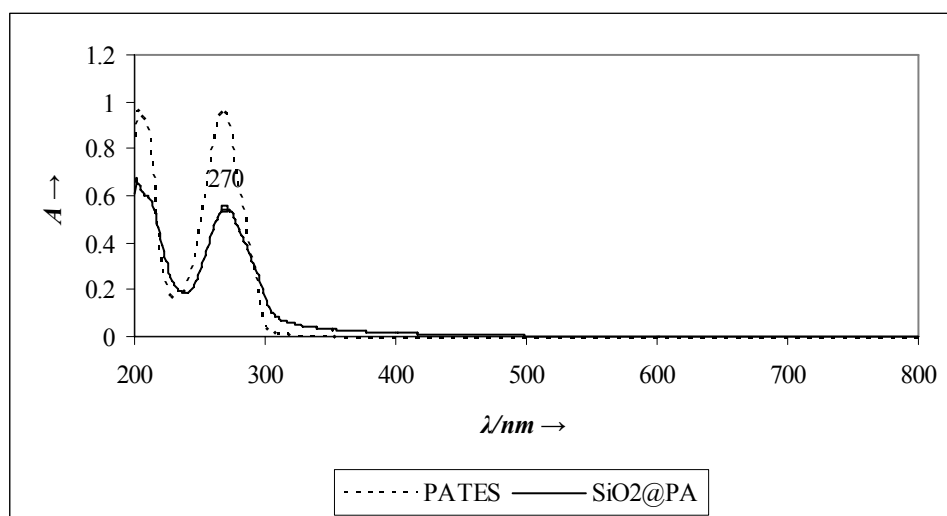


Figure 10. UV/Vis spectra of the 1 (PATES) and SiO₂@PA NPs

FT-IR spectra:

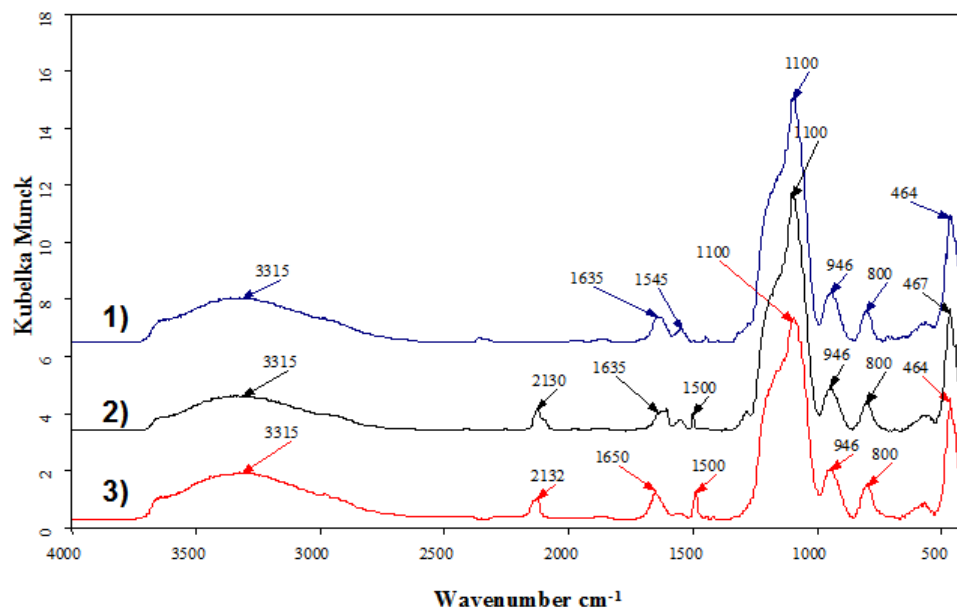


Figure 11. FTIR spectra of 1) SiO₂@BPh, 2) SiO₂@PA, and 3) SiO₂@PFPA NPs

S14

Size distribution graphs (according to TEM):

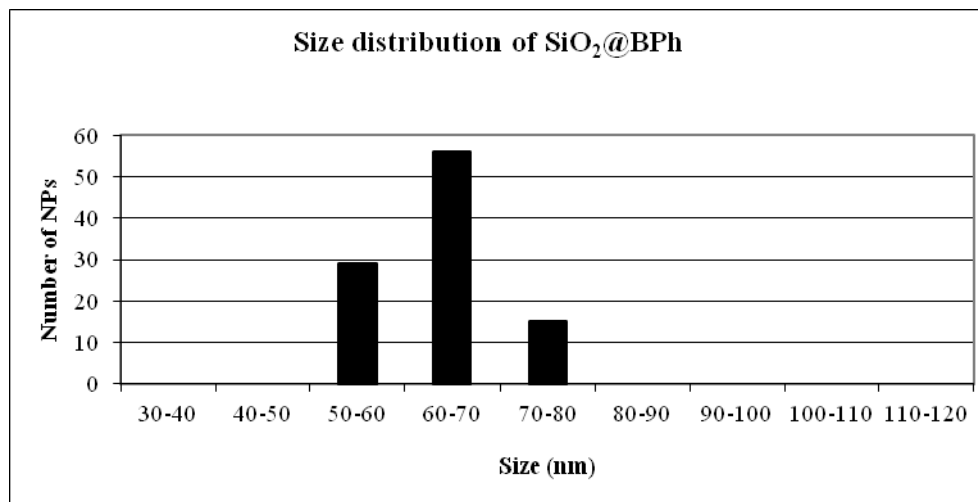


Figure 12. Size distribution of the SiO₂@BPh NPs

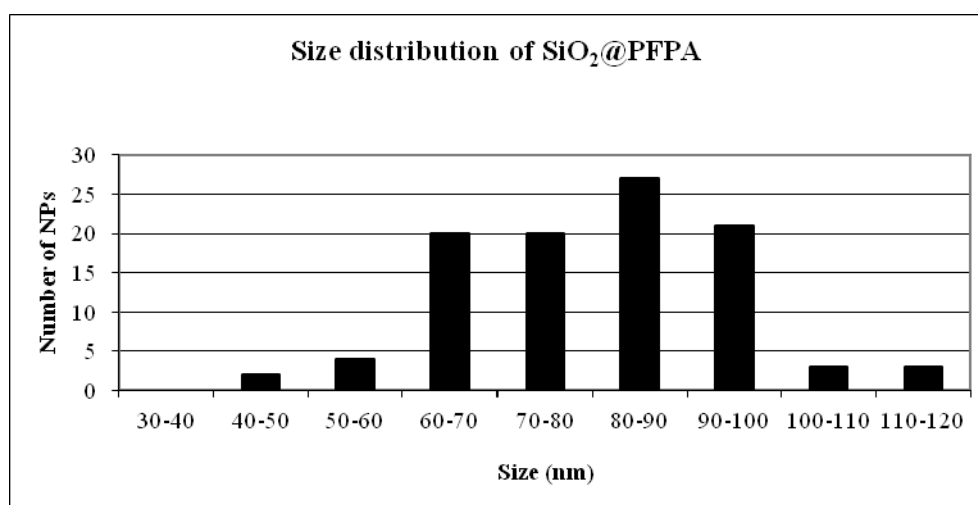


Figure 13. Size distribution of the SiO₂@PFPA NPs

S15

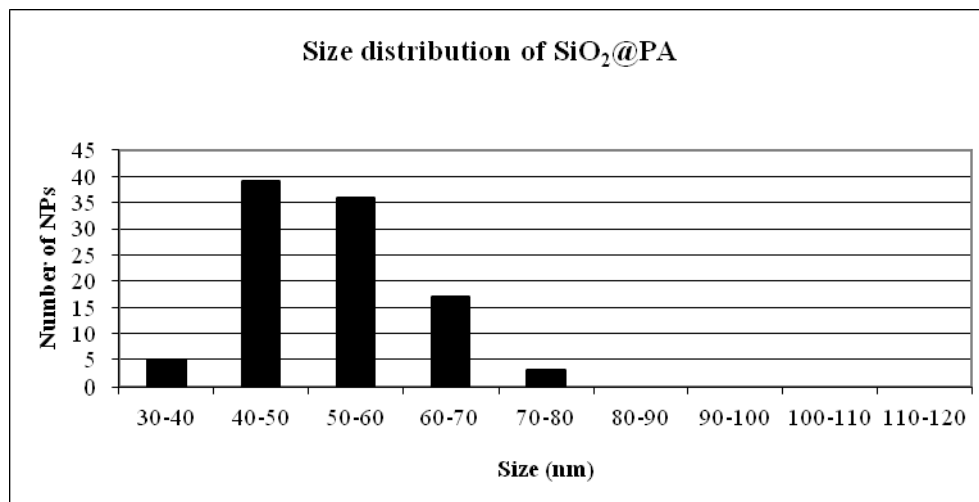


Figure 14. Size distribution of the SiO₂@PFPA NPs

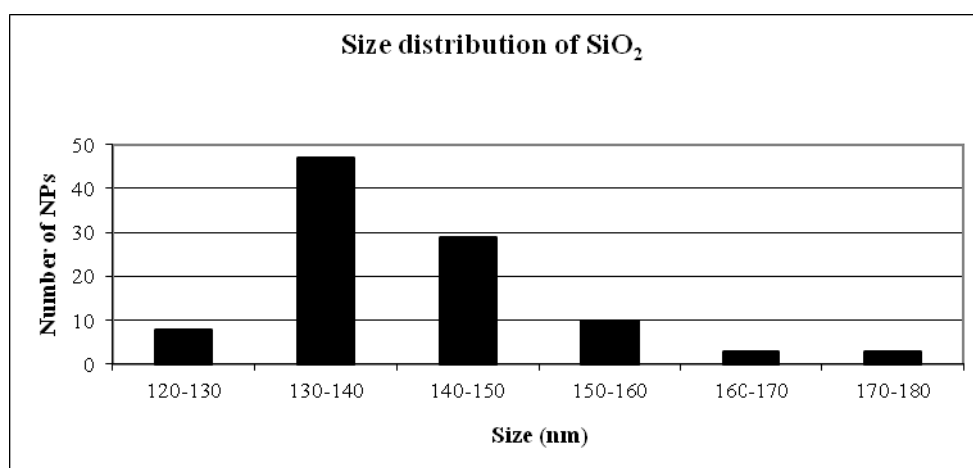


Figure 15. Size distribution of the SiO₂ NPs

S16

SEM tilt images:

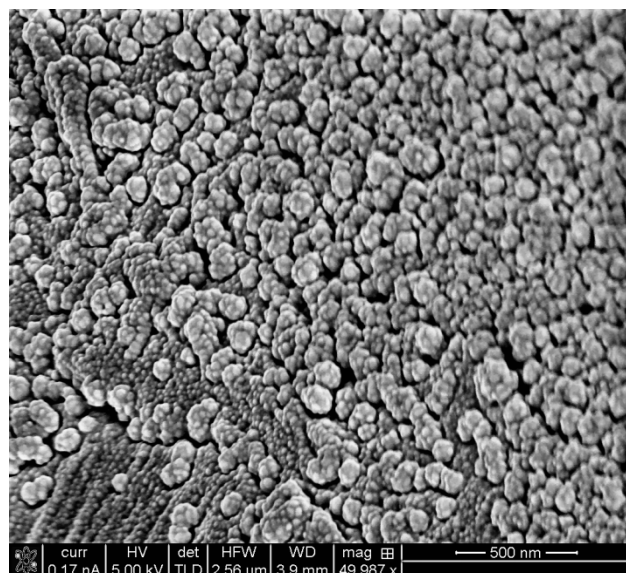


Figure 16. SEM tilt image of PC-SiO₂@PA film

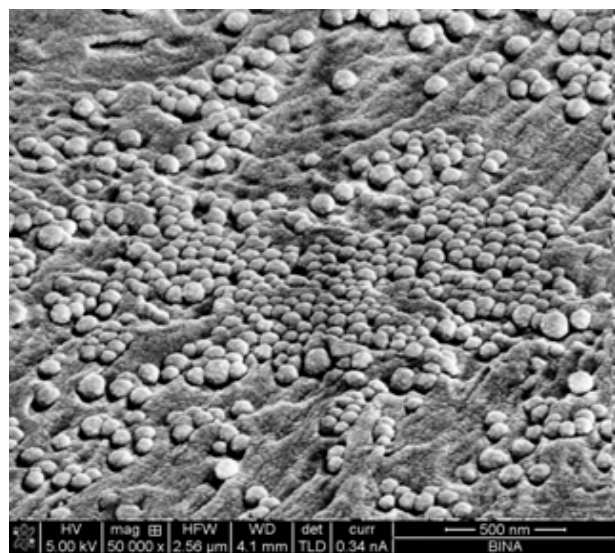


Figure 17. SEM tilt image of PC-SiO₂@PFPA film

S17

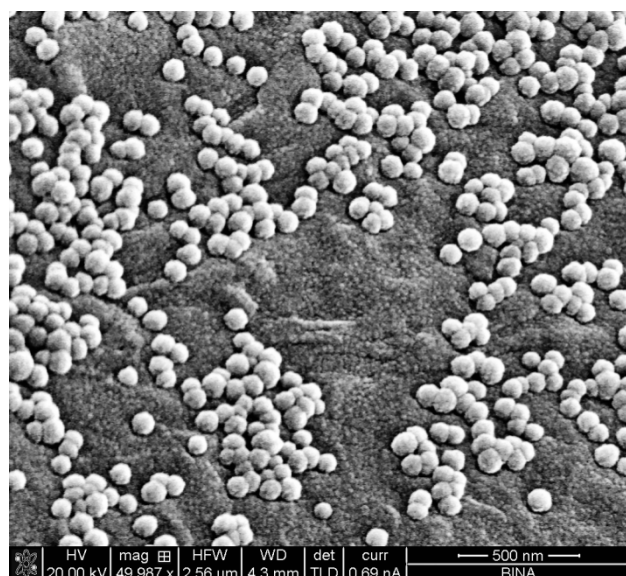


Figure 18. SEM tilt image of PC-SiO₂@BPh film

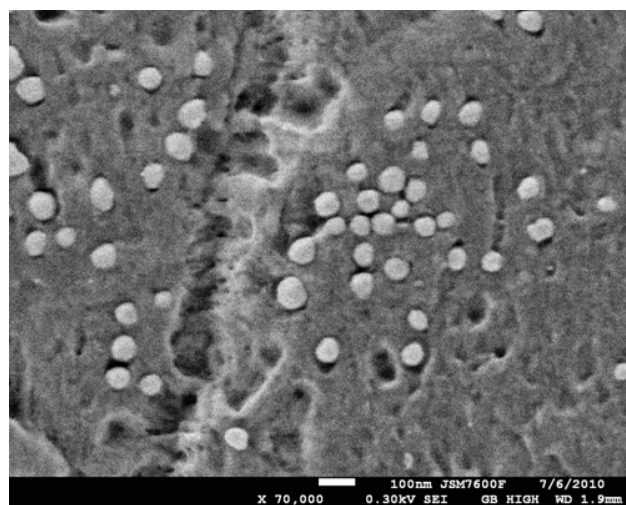


Figure 19. FE-SEM image of PC-SiO₂@PFPA modified film (the analysis was performed without gold conducting coating)

S18

AFM images:

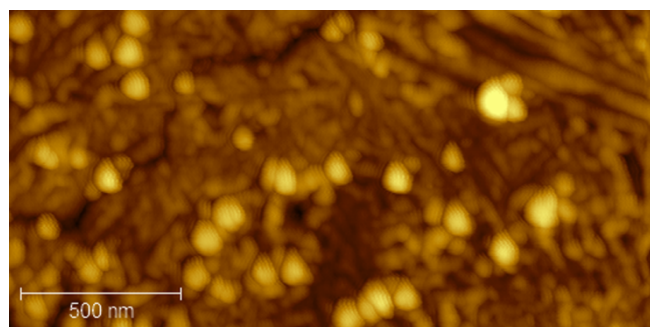


Figure 20. AFM image of PC-SiO₂@PA film

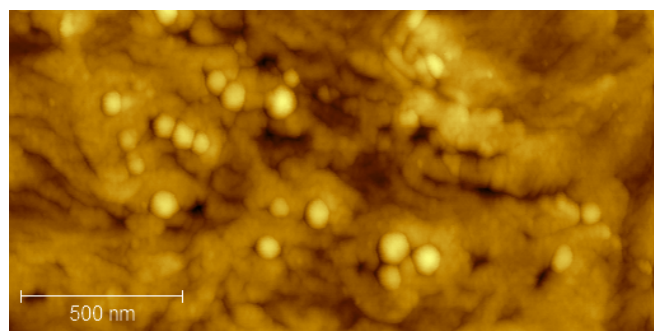


Figure 21. AFM image of PC-SiO₂@PFPA film

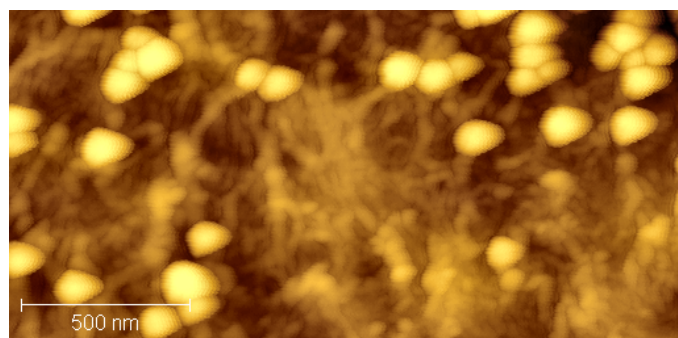


Figure 22. AFM image of PC-SiO₂@BPh film

AFM NP manipulation images:

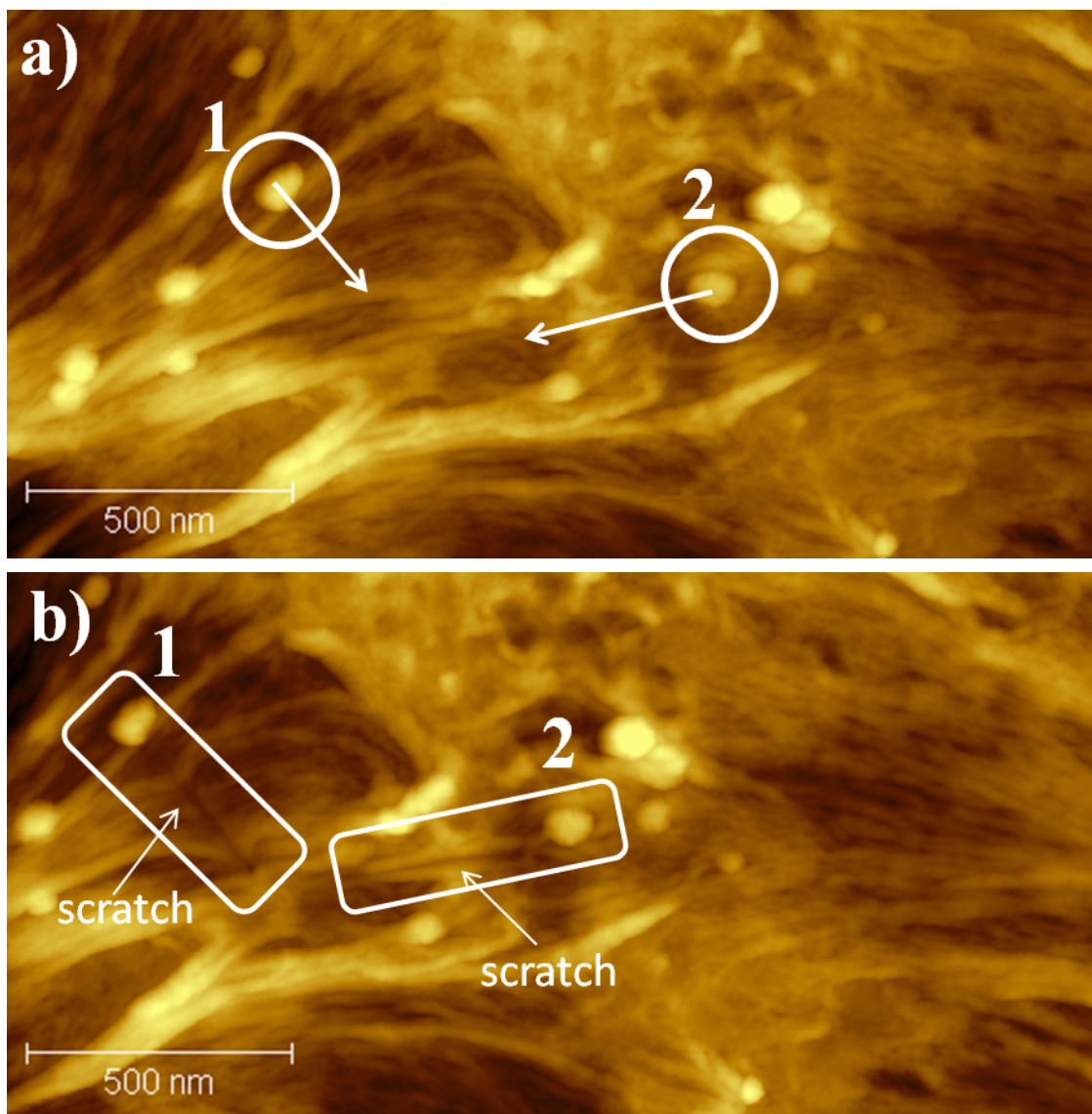


Figure 23. AFM image of PC-SiO₂@PA film : a) before and b) after NP manipulations. Particle 1 was moved with vertical tip depth of $Z = -40\text{nm}$ and particle 2 with $Z = -30\text{nm}$ both particles did not moved and scratches can be seen for both cases.

S20

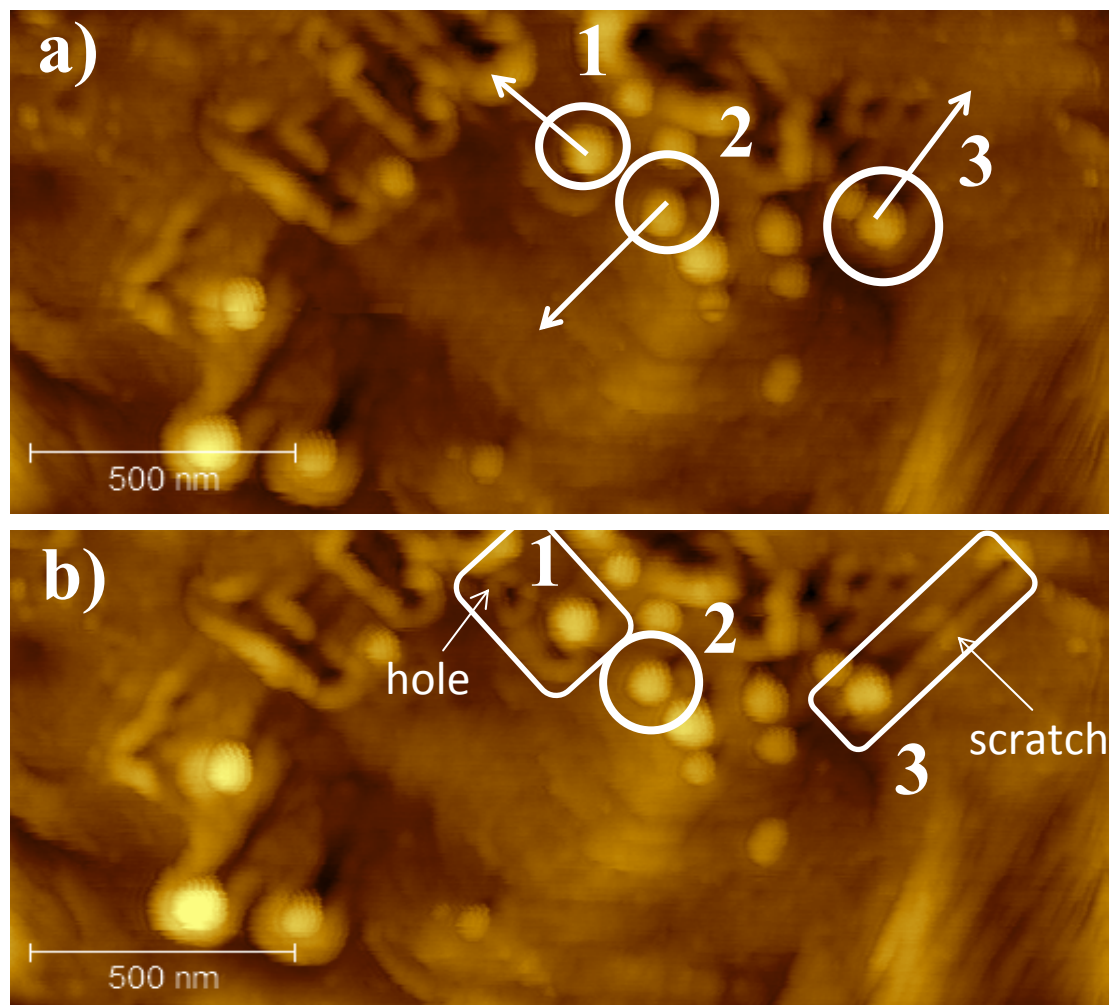


Figure 24. AFM image of PC-SiO₂@PFPA film : a) before and b) after NP manipulations. Particle **1** was moved with vertical tip depth of $Z = -20\text{nm}$ and $Z = -30$, particle **2** with $Z = -30\text{nm}$ and particle **3** with $Z = -40\text{nm}$ all three particles did not moved and a dip scratch can be seen for **3** and a hole in the place where the tip stopped for **2**.

S21

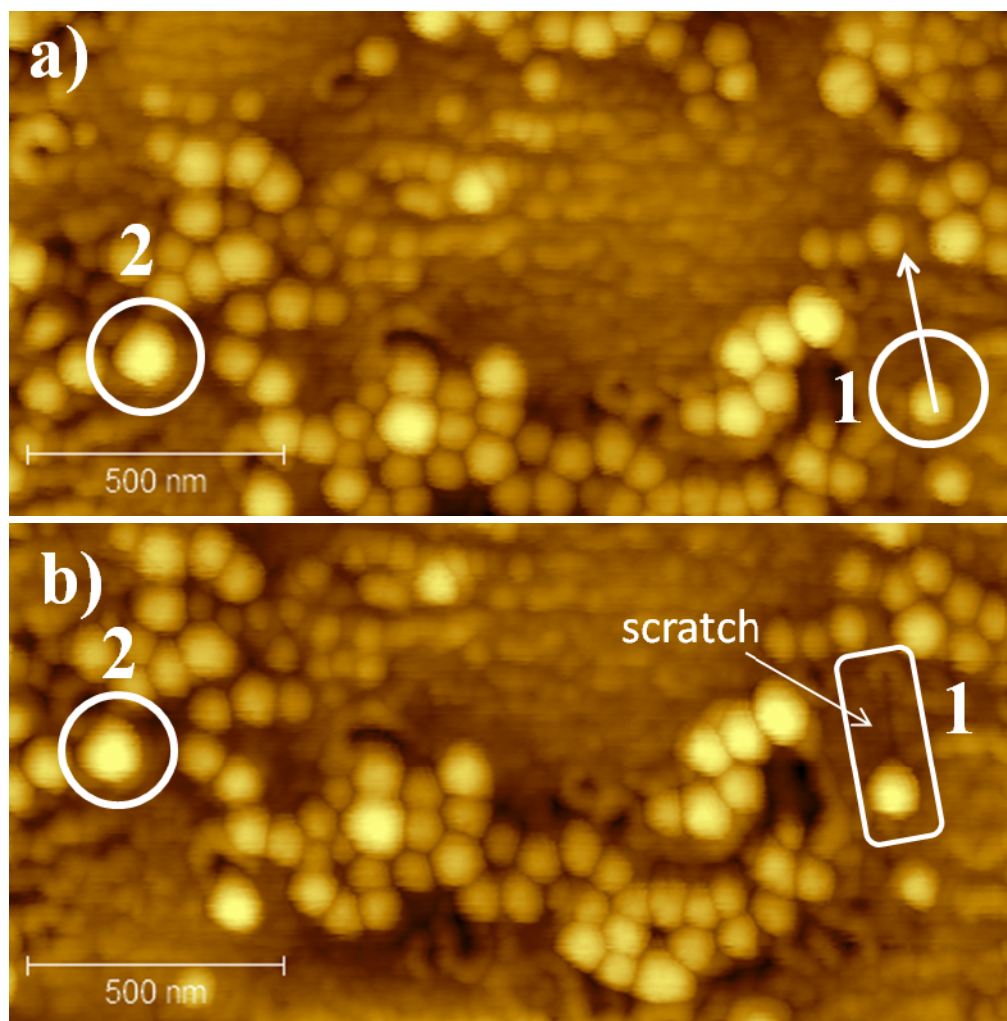


Figure 25. AFM image of PC-SiO₂@BPh film: a) before and b) after NP manipulations. Particle **1** was moved with vertical tip depth of Z = -30 and Z = -40nm and particle **2** with Z = -40nm, Z = -50nm and Z = -60nm both particles did not moved and scratch can be seen for **1**.

S22

Neat PC film

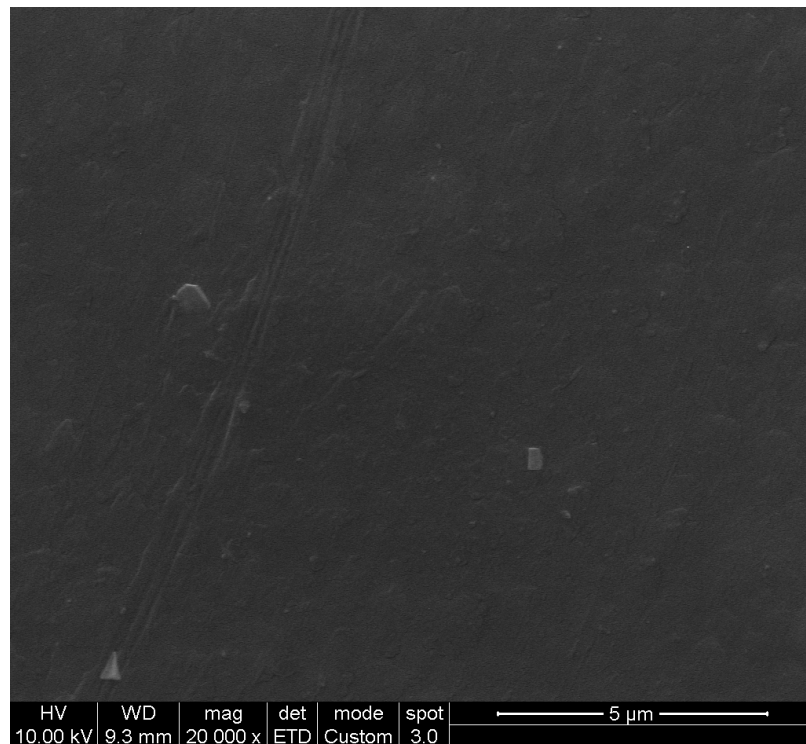


Figure 26. SEM image of neat PC film

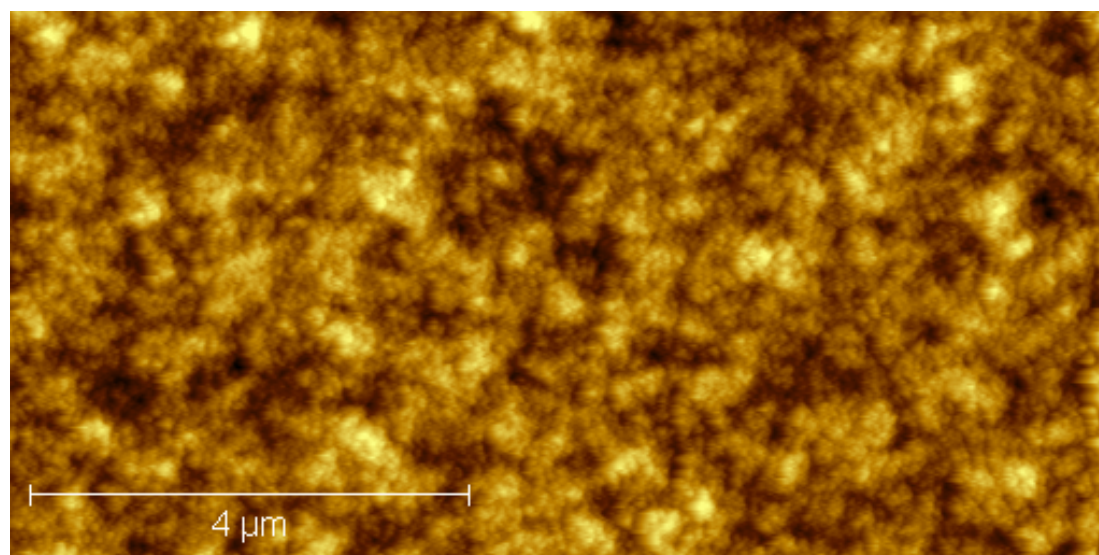


Figure 27. AFM image of neat PC film

S23

XPS spectra:

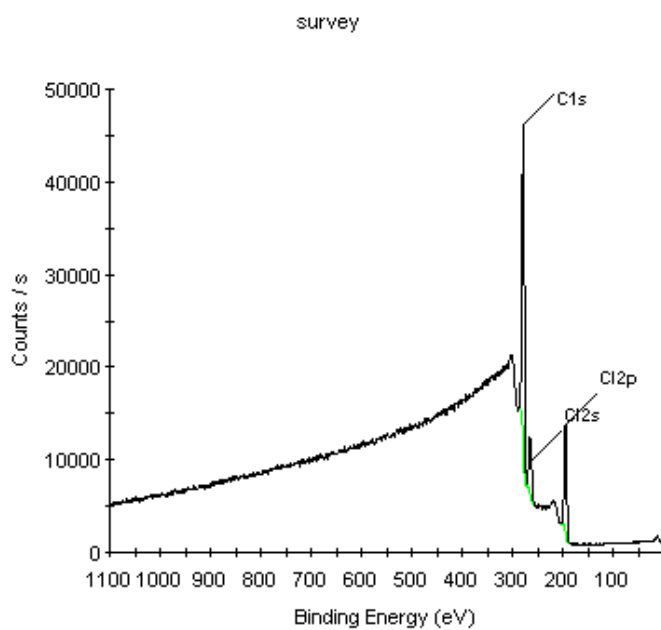


Figure 28. XPS spectra of neat PC film

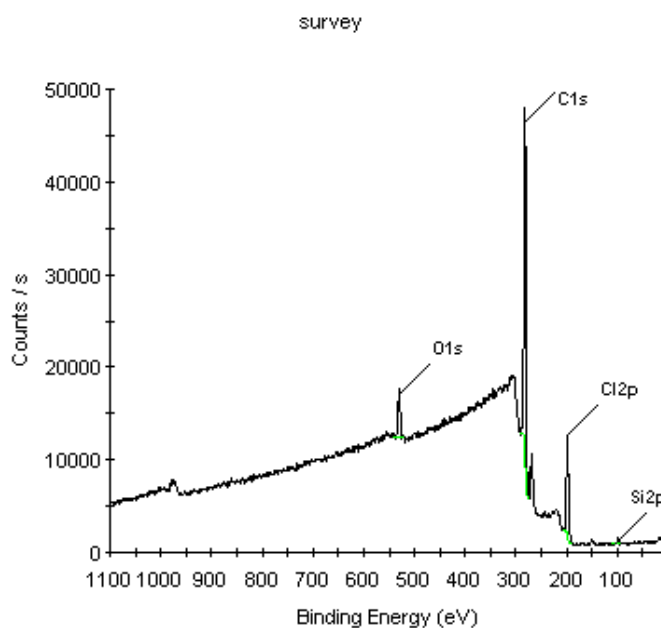


Figure 29. XPS spectra of PC-SiO₂ film

S24

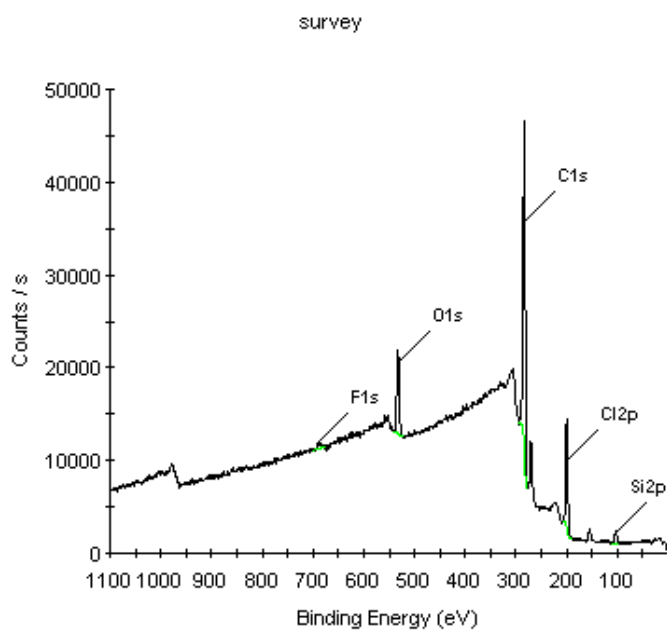


Figure 30. XPS spectra of PC-SiO₂@PFPA film

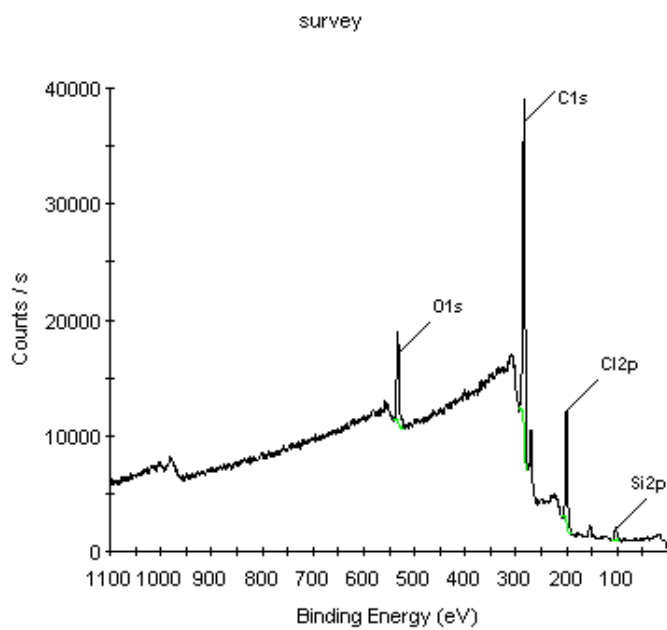


Figure 31. XPS spectra of PC-SiO₂@BPh film

S25

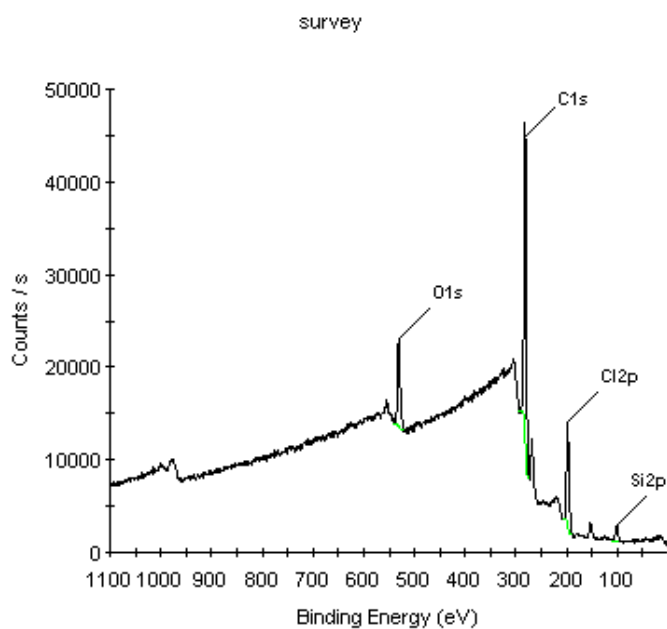


Figure 32. XPS spectra of PC-SiO₂@PA film

S26

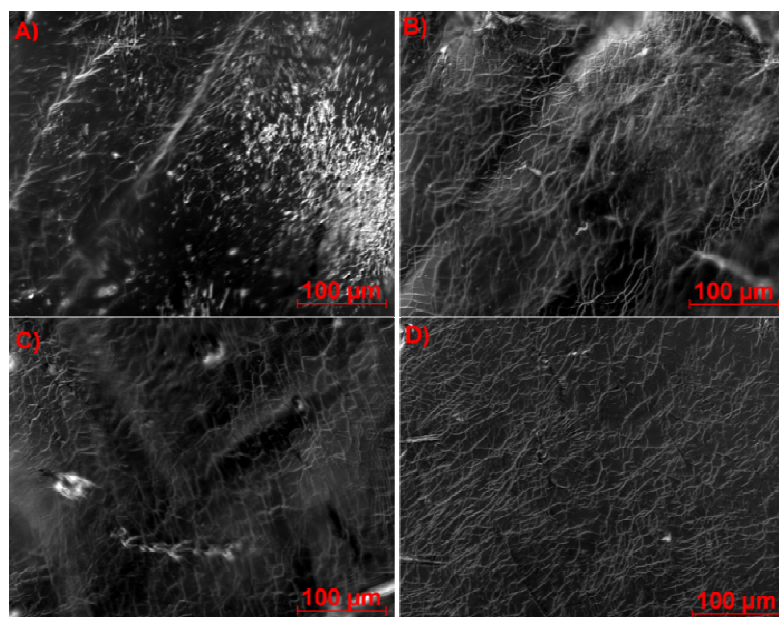


Figure 33. DIC filter images of A) PC-SiO₂@PA ; B) PC-SiO₂@PFPA; C) PC-SiO₂@BPh, and D) PC-SiO₂ films

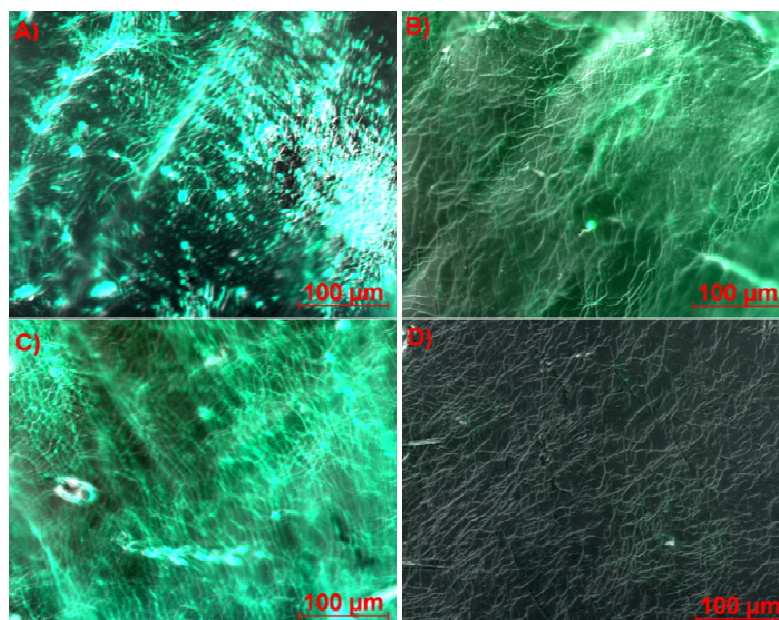


Figure 34. merged GFP, CFP, and DIC filters fluorescence images of A) PC-SiO₂@PA ; B) PC-SiO₂@PFPA; C) PC-SiO₂@BPh, and D) PC-SiO₂ films

Literature:

- [1] J. F. W. Keana, S. X. Cai, *J. Org. Chem.* **1990**, *55*, 3640-3647.
- [2] K. G. Pinney, J. A. Katzenellenbogen, *J. Org. Chem.* **1991**, *56*, 3125-3133.
- [3] H. Li, G. McGall, *Frontiers in Biochip Technology*, Springer, **2006**.